

# High-Impedance Wideband Folded Dipole Antenna for Energy Harvesting Applications

Hiroshi Miyagoshi, Keisuke Noguchi, Kenji Itoh, and Jiro Ida  
Kanazawa Institute of Technology, 7-1, Ogioka, Nonoichi, Ishikawa 921-8501, Japan

**Abstract** – A high-impedance wideband folded dipole antenna (FDA) has been designed for energy harvesting applications. High impedance is necessary for producing high efficiency rectennas. An impedance of over  $300 \Omega$  can be achieved by FDAs due to the impedance step-up function. The wideband design is introduced theoretically using an equivalent circuit for the FDA. A bandwidth over 20% with a characteristic impedance of  $350 \Omega$  was achieved. Measurements of the fabricated antenna are compared with the results of simulations and the high-impedance wideband design is verified.

**Index Terms** —digital TV broadcasting, energy harvesting, folded dipole antenna, high impedance, wideband.

## I. INTRODUCTION

Energy harvesting of digital TV (DTV) broadcasting radio waves has the potential to serve as a power supply for the terminals of sensor networks. High-efficiency rectennas are needed for such energy harvesting systems, for which we have proposed circuit topologies [1]. Furthermore, we investigated antennas with high impedance, as required by the rectifiers, and wideband characteristics adapted to the bandwidth of DTV [2].

A FDA is generally used as the feed element for a Yagi-Uda antenna receiving DTV signals. FDAs have a simple structure, low loss and an impedance step-up function. A wideband design for the FDA is needed in the case of higher-impedance antennas, although in general FDAs already have wideband characteristics.

In this paper, we present an FDA design that achieves an impedance of over  $300 \Omega$  and has wideband characteristics that cover the bandwidth of DTV. The FDA is designed theoretically using an equivalent circuit and the maximum bandwidth is predicted. A comparison is made between the results of a simulation and measurements of a fabricated FDA, and the characteristics of the FDA are discussed.

## II. ANTENNA MODEL AND THEORETICAL BANDWIDTH

A schematic diagram of the FDA is shown in Fig. 1. The FDA consists of two conductors printed on both sides of a dielectric substrate. The size of the substrate is  $283\text{mm} \times 25\text{mm} \times 1\text{mm}$ . Both conductors are connected via a hole in the dielectric that is located at a quarter wavelength from the feed point.

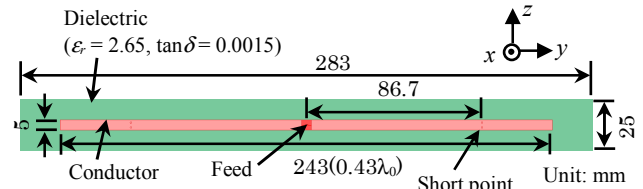


Fig. 1. Folded dipole antenna (FDA).

Fig. 2 shows an equivalent circuit for the FDA. The circuit is composed of a transformer that performs a step-up function, a radiation impedance  $Z_r$  and a transmission-line impedance  $Z_b$ . The impedance  $Z_r$  provides series resonance equal to that of a normal half-wavelength dipole antenna. On the other hand, the impedance  $Z_b$  provides parallel resonance at the operating frequency. We express these impedances as

$$Z_r = R + jRQ \left( \frac{f}{f_0} - \frac{f_0}{f} \right) \quad (1)$$

$$Z_b = jZ_0 \tan \beta \ell \quad (2)$$

where  $R$ ,  $Q$  and  $f_0$  denote the radiation resistance, the quality factor and the resonant frequency, respectively.  $Z_0$ ,  $\beta$  and  $\ell$  are the characteristic impedance, the phase constant and the length of the transmission-line with respect to the folded structure of the FDA, respectively. We can express the input impedance  $Z_{in}$  as follows.

$$Z_{in} = \frac{2n^2 Z_r Z_b}{n^2 Z_r + 2Z_b} \quad (3)$$

We derived the maximum bandwidth  $BW$  of the FDA using equations (1) – (3) [3].

$$BW = \frac{\sqrt{\rho^2 - 1}}{Q} \quad (4)$$

Here,  $\rho$  represents the maximum allowable VSWR. We predicted the bandwidth of the FDA using (4); the results are shown in Fig. 3. When the value of the  $Q$  factor for the FDA is from 5 to 8, a bandwidth greater than 20% is achieved with the VSWR = 2 criterion.

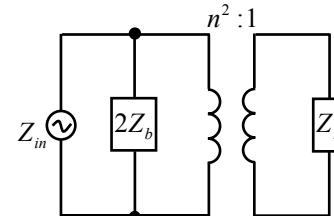


Fig. 2. Equivalent circuit for FDA.

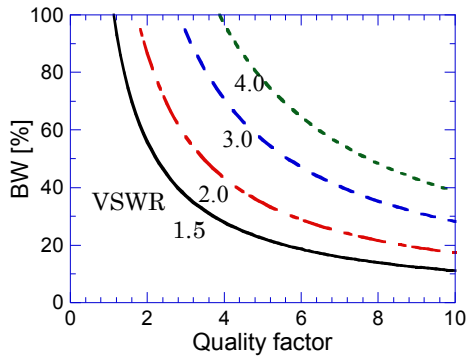


Fig. 3. Maximum bandwidth versus  $Q$  factor for different maximum allowable VSWRs.

### III. CHARACTERISTICS OF FDA

The simulated and measured impedance characteristics and VSWRs are shown in Figs. 4 and 5. The simulation was performed using a full wave EM simulator, Agilent EM Pro 2012. In these figures, the characteristic impedance  $Z_c$  of the feed lines is assumed to be  $350 \Omega$ . As seen in Fig. 4, wideband characteristics were obtained that show the locus of impedance having a kink at the center of the Smith chart. The VSWR plot shown in Fig. 5 also indicates wideband characteristics and a measured bandwidth of 112.8 MHz (21.1% for the operating frequency of 535 MHz) was obtained with the  $VSWR = 2$  criterion. The bandwidth covers the main range of the DTV band.

Radiation patterns at the lowest, operating and highest frequencies are shown in Fig. 6. These patterns are the co-polarization component of  $E_\phi$  in  $xy$ -plane. At all frequencies, figure of eight-shaped patterns are observed. The simulated and measured results are in good agreement with each other. In the simulation, the gain is 2 dBi in the  $x$  direction.

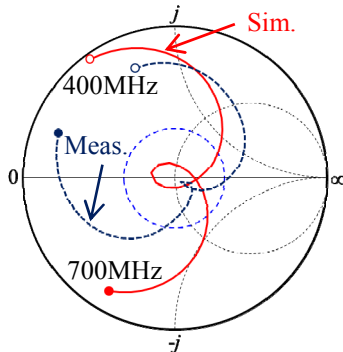


Fig. 4. Impedance characteristics.

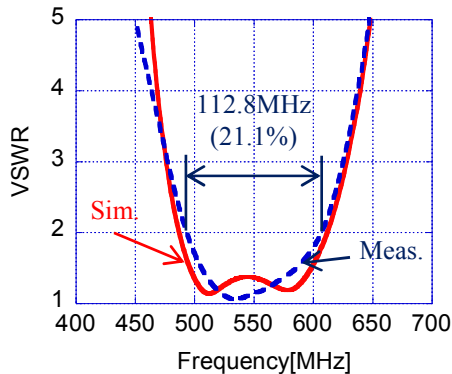


Fig. 5. VSWR.

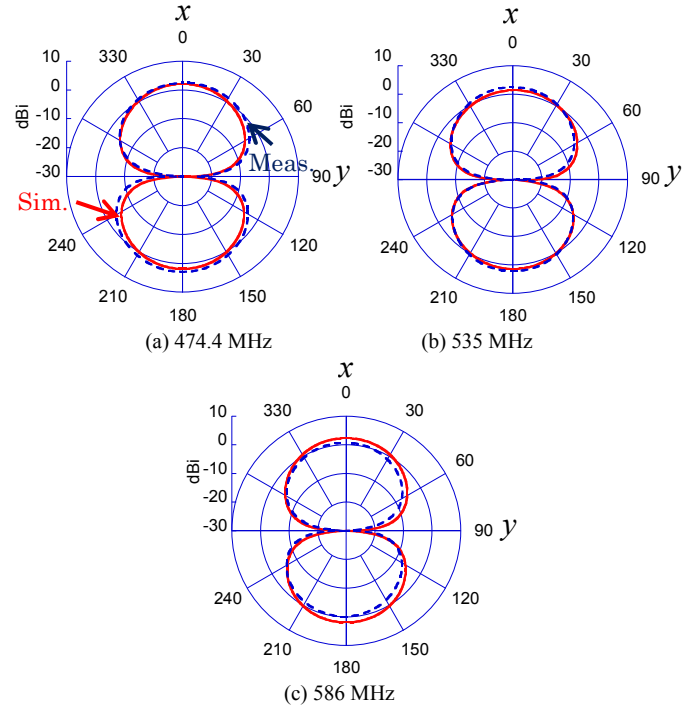


Fig. 6. Radiation pattern.  $xy$ -plane,  $E_\phi$ .

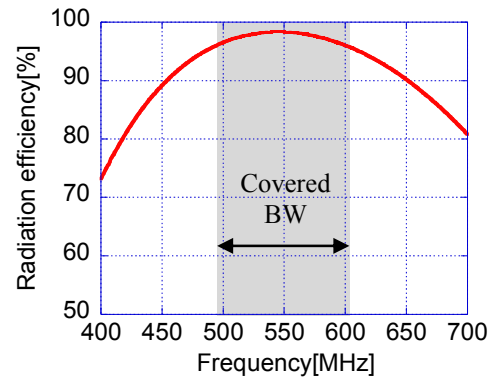


Fig. 7. Radiation efficiency.

The radiation efficiency was estimated in the simulation, and the results are shown in Fig. 7. An efficiency of 95-98% was achieved in the operating frequency range.

### IV. CONCLUSION

A folded dipole antenna was designed to obtain high impedance and wideband characteristics for high-efficiency rectennas for energy harvesting applications. The theoretical bandwidth calculated from the equivalent circuit was over 20% with the  $VSWR = 2$  criterion. Furthermore, a bandwidth of 21.1% for a characteristic impedance of  $350 \Omega$  was achieved. Figure of eight-shaped radiation patterns were obtained across the entire bandwidth.

### REFERENCES

- [1] M. Ioth, et al., IEEE WPTC 2014, pp.64-67, May, 2014.
- [2] H. Miyagoshi, et al., STARC symposium 2014, No.29, Jan., 2014.
- [3] K. Noguchi, et al., IEEE AP-S 2013, pp.766-767, July, 2013.
- [4] R. Umesao, et al., IEEE FTFC 2014, pp.4.5.1-4.5.4, Mar., 2014.